IEEE Access
Multidisciplinary | Rapid Review | Open Access Journal

Received October 24, 2019, accepted November 23, 2019, date of publication November 29, 2019,
date of current version December 13, 2019.

Digital Object Identifier 10.1109/ACCESS.2019.2956825

Multiple Sources Localization by the WSN Using the Direction-of-Arrivals Classified by the Genetic Algorithm

YUAN ZHANG AND YUE IVAN WU, (Senior Member, IEEE)
College of Computer Science, Sichuan University, Chengdu 610065, China

Corresponding author: Yue Ivan Wu (y.i.wu@ieee.org)

This work was supported in part by the National Natural Science Foundation of China (NSFC) under Grant 61401291, in part by the Sichuan Science and Technology Program under Grant 2019YFG0118, and in part by the Chengdu Science and Technology Program under Grant 2019-YF05-00998-SN.

ABSTRACT Simultaneously locating multiple sources passively in the wireless sensor networks (WSN) is challenging in the internet of things (IoT) applications, where reducing the computation and communication load is of great importance due to the requirement on real-time processing and the energy constraint. This is especially true when the number of sources or the number of sensor nodes is large. In this paper, a localization algorithm to estimate multiple sources' positions in the three-dimensional space is proposed. With the direction-of-arrival (DOA) estimates for multiple sources obtained at each sensor node, it is crucial to discriminate which estimate corresponds to which source. To save the computation resources, a classification method based on the genetic algorithm is proposed to handle the multiple sources. A fitness function is designed to assess the clustering of the DOA estimates. Extensive simulations are carried out to analyze the algorithm performance under the various settings. Numerical examples show that the proposed method could lower the computational burden by orders of magnitude compared to the conventional method, without significantly sacrificing the estimation accuracy.

INDEX TERMS Direction-of-arrival, genetic algorithm, multiple sources localization, triangulation, wireless sensor network.

I. INTRODUCTION

Wireless sensor networks (WSN) have been widely applied in both civilian and military applications, especially with the advancement of internet of things (IoT) in recent years. The data obtained by the sensors are informative only when the physical locations are associated. As many applications demand the awareness of source positions, the localization of unknown sources with the WSN has drawn vast of attentions. Unlike many conventional WSN implementations of locating only a single source, the application scenarios of IoT usually require to locate multiple passive sources in three-dimensional space simultaneously. Extending the localization to handle multiple sources is nontrivial, as many existing methods for single source localization would fail to work. One should be noted that many previous works in the literature, such as [19], [25], [24], [27], [33], and [34], discuss the self-localization problem where the to-be-located sources are cooperative sensor nodes in the WSN. This is fundamentally different from the concern of this paper. In scenarios such as maritime surveillance, aerospace tracking, biotic herd monitoring, and etc, the interested sources are often non-cooperatively "passive" sources, providing barely any prior knowledge or cooperation to the WSN. Another common feature in the IoT applications is the large number of deployed sensor nodes, which would result heavy computation burden and energy consumption for data fusion. In such scenarios, the localization task becomes even more challenging. To efficiently and reliably locate multiple sources becomes an extremely appealing task, which is not fully explored in the literature [32].

Depending on the measurements, the conventional localization algorithms for multiple sources in the literature can be roughly classified into the following categories: (1) the Global Positioning System (GPS) [4], (2) the directly received data [2], [6], [22], [26], [28], (3) the received signal

The associate editor coordinating the review of this manuscript and approving it for publication was Rongbo Zhu.

strength (RSS) [10], [8], [17], [23], [29], (4) the time-of-arrival (TOA) or the time-difference-of-arrival (TDOA) [30], [35] and (5) the direction-of-arrival (DOA) [18], [36]. For a more detailed survey on the existing methods, one may refer to [12], [14], and [32].

The GPS method is well known for its high accuracy in localization. However, the GPS may be inapplicable to many IoT scenarios because it is energy consuming and inefficient in enclosed environment such as indoor and tunnel. The localization scheme based on directly received data usually involves either maximum likelihood estimation (MLE) [2], [6], [22] or steer response power (SRP) evaluation [26], [28], both resulting huge communication load at the sensor nodes, as well as the heavy computation load at the fusion center. The RSS based methods are simple and economic as no auxiliary hardware is required at each sensor node. However, the RSS based methods often depend on the prior knowledge of the attenuation model of the propagation channel which may not be available in applications. Moreover, many RSS methods are either uncompetitive to handle multiple sources [31], or involving sophisticated iterative algorithms unsuitable for IoT applications [10], [8], [17], [23], [29]. The TOA/TDOA based methods generally provide reasonable high accuracy of localization. But their performances severely degrade when locating multiple sources. It also requires critical time synchronization between the sensor nodes. The DOA based methods often work in a semi-distributed manner, which is efficient for communication between the sensor nodes, requiring neither the channel parameters nor the inter-node synchronization. The major problem is that they are traditionally considered power hungry with large dimensions, because the sensor array is usually attached to each node. Fortunately, the directional sensor nodes nowadays can be compactly and economically implemented thanks to the recent development of the micro-electromechanical systems (MEMS) [11], [13], [15], [16].

Recently, an efficient multiple sources localization scheme is proposed in [36]. With all the DOA estimates obtained at the sensor nodes, a classification process is proposed to associate each estimate with the corresponding source. This classification is modeled as an optimization problem, and solved by the brute force search in the sense of least square error (LSE). However, the computation load of [36] dramatically increases as the number of nodes/sources increases. To solve this problem, a data fusion strategy is proposed in this work. By taking into account the statistical distribution of the DOA estimates at the sensor nodes, a classification procedure is formulated using the essentials of an evolutionary process, and optimized in the paradigm of genetic algorithm. After the DOA classification, the multiple sources can be simultaneously located in the three-dimensional space. Unlike that [36] is capable of finding the global optimum of the classifications on the DOA estimates, the proposed method is suboptimal due to the nature of the genetic algorithm. Thus, [36] is utilized as a benchmark of estimation accuracy to the proposed algorithm. The numerical comparison shows that the proposed localization method has orders of magnitude lower computational burden, without severely sacrificing the estimation accuracy.

Another advantage is, the proposed localization algorithm would not put challenge on the WSN's energy consumption and control overhead, since the computation in the proposed scheme is centralized. The DOA classification and the sources localization are implemented at the data processing center, but not at the sensor nodes. Only a few scalars (the DOA estimates) instead of the raw data are required to be transmitted, which greatly reduces the communication load between the sensor nodes and the center. The proposed localization algorithm is not directly related to the general definitions of the network lifetime, such as the sensor node failure, power consumption, coverage, connectivity and etc, though the aforementioned metrics could be important in practice.

The following parts of this paper are organized as follows. Section II formulates the problem and data model. Section III proposes a DOA classification method based on genetic algorithm to handle multiple sources. Section IV proposes the localization method with the results obtained in Section III. Section V summarizes the proposed algorithm. Section VII presents the numerical examples showing the efficacy of the proposed method. Section VIII concludes the paper.

II. PROBLEM FORMULATION

Assume M sensor nodes locating at $\mathbf{p}_m = [x_m, y_m, z_m]^T$ for $m = 1, \ldots, M$, and L sources locating at $\mathbf{q}_\ell = [x_\ell, y_\ell, z_\ell]^T$ for $\ell = 1, \ldots, L$. Define the unitary direction vector pointing from $\mathbf{p}_m$ to $\mathbf{q}_\ell$ as $\mathbf{u}_{m,\ell}$, with the elevation angle $\theta_{m,\ell} \in [0, \pi]$ measured from the positive z-axis, and the azimuth angle $\phi_{m,\ell} \in [0, 2\pi)$ measured from the positive x-axis, as shown in Figure 1. Thus, the unitary direction vector from the m-th sensor to the ℓ-th source can be represented as

$$\mathbf{u}_{m,\ell} = [\sin\theta_{m,\ell}\cos\phi_{m,\ell}, \sin\theta_{m,\ell}\sin\phi_{m,\ell}, \cos\theta_{m,\ell}]^T. \quad (1)$$

Suppose that each sensor node in the WSN is capable of estimating the DOA of the L sources with respect to itself.[1] With multiple independent measurements, the estimates of the elevation angle and the azimuth angle can be modeled as

$$\begin{cases} \hat{\theta}_{m,\ell} = \theta_{m,\ell} + n_\theta \\ \hat{\phi}_{m,\ell} = \phi_{m,\ell} + n_\phi, \end{cases} \quad (2)$$

where $n_\theta \sim N(0, \sigma_\theta^2)$ and $n_\phi \sim N(0, \sigma_\phi^2)$ are angular errors modeled as zero mean Gaussian random variables [5], [20], with variances $\sigma_\theta \ll \frac{\pi}{2}$ and $\sigma_\phi \ll \pi$, respectively.

Inserting $\hat{\theta}_{m,\ell}$ and $\hat{\phi}_{m,\ell}$ into (1), the estimates of the unitary direction vector $\hat{\mathbf{u}}_{m,\ell}$ can be obtained. The estimated DOA

[1] The DOA estimates can be obtained by direction finding with sensor array at each sensor node [15], [18], or by measuring the received signal strength with directional sensor [16], [21]. To avoid the unnecessary distraction, the exact estimator used at each sensor node is not within the scope of our current investigation, as it does not affect the proposed algorithm.

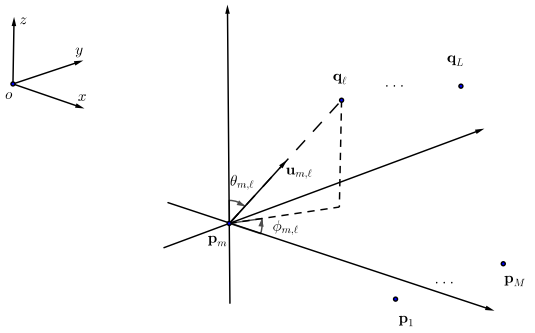

FIGURE 1. *L* sources and *M* sensor nodes in the three dimensional Cartesian coordinates system.

of $\mathbf{q}_\ell$ with respect to $\mathbf{p}_m$ can be defined by a directional ray $\left\{\mathbf{p}_m, \hat{\mathbf{u}}_{m,\ell}\right\}$. The objective is to estimate all source positions $\hat{\mathbf{q}}_\ell$, given the $M \times L$ directional rays $\left\{\mathbf{p}_m, \hat{\mathbf{u}}_{m,\ell}\right\}$, where $m = 1, \ldots, M$, and $\ell = 1, \ldots, L$.

III. DOA CLASSIFICATION WITH GENETIC ALGORITHM

In the noiseless case, there would be M directional rays $\left\{\mathbf{p}_m, \hat{\mathbf{u}}_{m,\ell}\right\}, \forall m$ intersecting exactly at the source locations $\mathbf{q}_\ell$, for each of the specific ℓ. In the noisy case, these M directional rays are generally skew in the three dimensional space. Despite not intersecting, they would likely be close to each other around the source, if the signal to noise ratio (SNR) is sufficiently high. Thus, correctly deciding the M directional rays associated with $\mathbf{q}_\ell$ is essential to locating the sources.

To classify all the $M \times L$ directional rays into L groups, each containing M directional rays starting at M sensor nodes, there are L^M possible classifications in total. To find the correct classification of directional rays associated with L sources, [36] traverses all possible classifications with a cost function in the sense of LSE. Since the number of possible classifications increases exponentially against the number of sensor nodes M, this method could result huge computation load.

Proposed in this Section is a classification process based on the genetic algorithm. The genetic algorithm is well known as a probabilistic search method suitable to a variety of combinatorial optimization problems by simulating the natural evolutionary process [1]. The individuals who are more successful in adapting to the environment will have a better chance to survive during the population evolution. On the other hand, the individuals who are not adapted to the environment will be eventually eliminated. The genes of the highly fit individuals will spread to a large amount of descendants, such that the whole population will finally be more adapted to the environment.

The aforementioned directional rays classification problem is formulated with the paradigm of genetic algorithm using the following essentials.

A. ENCODING

Define an L-nary code of M bits, i.e., a *chromosome*, as

$$\mathbf{c} \triangleq [[\mathbf{c}]_1, [\mathbf{c}]_2, \cdots, [\mathbf{c}]_M]^T, \tag{3}$$

where the m-th bit $[\mathbf{c}]_m \in \{1, \ldots, L\}$ represents the directional ray $\left\{\mathbf{p}_m, \hat{\mathbf{u}}_{m,[\mathbf{c}]_m}\right\}$.

For some specific $[\mathbf{c}]_1 = \ell$, listing all possible $\mathbf{c}$ as columns defines an $M \times L^{M-1}$ *chromosome matrix*

$$\mathbf{C}_\ell \triangleq \begin{bmatrix} \ell & \ell & \ldots & \ell & \ell \\ 1 & 1 & \ldots & L & L \\ \vdots & \vdots & \vdots & \vdots & \vdots \\ 1 & 2 & \ldots & L-1 & L \end{bmatrix}_{M \times L^{M-1}}, \tag{4}$$

where each column of $\mathbf{C}_\ell$ is called an *individual*, carrying the indexes of M directional rays.

In the above $\mathbf{C}_\ell$, the number ℓ on the first row signifies the current source of interest for DOA classification. Through the algorithm described in the later Sections III-B to III-E, this $[\mathbf{c}]_1 = \ell$ should remain unchanged, *unless* the source of interest changes. Initially, one could assume $[\mathbf{c}]_1 = 1$ without loss of generality.

B. FITNESS

To assess the closeness of M directional rays indexed specifically by $\mathbf{c}$, the following fitness function is proposed

$$f(\mathbf{c}) \triangleq \left[w_1 \underbrace{\sum_{i=2}^{M} d([\mathbf{c}]_1, [\mathbf{c}]_i)}_{\triangleq \Sigma_1} + w_2 \underbrace{\sum_{i=2}^{M} \sum_{j=i+1}^{M} d([\mathbf{c}]_i, [\mathbf{c}]_j)}_{\triangleq \Sigma_2} \right]^{-1}, \tag{5}$$

where $w_1 + w_2 = 1$, $w_1, w_2 \in [0, 1]$ denote the weights of the two summation terms Σ_1 and Σ_2. In equation (5),

$$d([\mathbf{c}]_i, [\mathbf{c}]_j) \triangleq \min \left\| \left(\mathbf{p}_i + k_i \hat{\mathbf{u}}_{i,[\mathbf{c}]_i}\right) - \left(\mathbf{p}_j + k_j \hat{\mathbf{u}}_{j,[\mathbf{c}]_j}\right) \right\|, \quad i \neq j, \quad \text{subject to} \quad k_i \geq 0 \quad \& \quad k_j \geq 0 \tag{6}$$

denotes the minimum distance between the directional rays $\left\{\mathbf{p}_i, \hat{\mathbf{u}}_{i,[\mathbf{c}]_i}\right\}$ and $\left\{\mathbf{p}_j, \hat{\mathbf{u}}_{j,[\mathbf{c}]_j}\right\}$. $\|\cdot\|$ signifies the Euclidean norm. In equation (6), the constraints $k_i \geq 0$ and $k_j \geq 0$ guarantee the distance is between two rays. Without these constraints, $d([\mathbf{c}]_i, [\mathbf{c}]_j)$ becomes the conventional definition of distance between two lines.

The M directional rays indexed by a chromosome $\mathbf{c}$ can be divided into two groups: (i) a single directional ray from the first sensor node, i.e., $\left\{\mathbf{p}_1, \hat{\mathbf{u}}_{1,[\mathbf{c}]_1}\right\}$, and (ii) the other $M-1$ directional rays. On the right hand side of equation (5), the first summation term Σ_1 calculates the sum of distances between (i) and each of (ii), assessing how close (ii) is to (i). The second summation term Σ_2 calculates the sum of distances between all possible pairs of the directional rays in (ii), assessing the "closeness" of the $M-1$ directional rays in (ii).

From equations (5) and (6), Σ_1 depends on the accuracy of the DOA estimate $\hat{\mathbf{u}}_{1,[\mathbf{c}]_1}$ at the first sensor node, while Σ_2 does not. If $w_1 > w_2$, $f(\mathbf{c})$ would be more likely to depend on the directional ray $\left\{\mathbf{p}_1, \hat{\mathbf{u}}_{1,[\mathbf{c}]_1}\right\}$, thus the estimation error of $\hat{\mathbf{u}}_{1,[\mathbf{c}]_1}$. On the other hand, if $w_1 < w_2$, $f(\mathbf{c})$ would be more likely to depend on the rest of $M-1$ directional rays. Thus, different weighting strategy can be applied. For example, by setting $w_1 = w_2 = \frac{1}{2}$, equation (5) degenerates to $f(\mathbf{c}) = 2(\Sigma_1+\Sigma_2)^{-1} = 2\left[\sum_{i=1}^{M}\sum_{j=i+1}^{M} d\left([\mathbf{c}]_i, [\mathbf{c}]_j\right)\right]^{-1}$, which puts identical weight on each of the M directional rays and has the highest computational complexity. By setting $w_1 = 1$ and $w_2 = 0$, equation (5) degenerates to $f(\mathbf{c}) = \Sigma_1^{-1}$, which weighs more on $\left\{\mathbf{p}_1, \hat{\mathbf{u}}_{1,[\mathbf{c}]_1}\right\}$ and has the lowest computational complexity. How the weighting strategy affects the proposed algorithm will be discussed in more details in Section VII-B.

C. SELECTION

Randomly selecting $K \leq L^{M-1}$ individuals (columns) from $\mathbf{C}_\ell$ in (4), denoted as $\mathbf{c}_1, \ldots, \mathbf{c}_K$, form a *generation* of chromosomes, whose corresponding fitness $f(\mathbf{c}_k)$ can be obtained by equation (5). Define the selection probabilities as

$$p(\mathbf{c}_k) \triangleq \frac{f(\mathbf{c}_k)}{\sum_{k=1}^{K} f(\mathbf{c}_k)}, \quad k = 1, \ldots, K \tag{7}$$

Thus, each individual $\mathbf{c}_k$ survives to the next generation with the probability $p(\mathbf{c}_k)$. This can be implemented by *roulette wheel selection* [3] using a random variable with uniform distribution, i.e, $\eta \sim U[0, 1]$. The next generation of individuals are selected by performing the following selection for K times:

$$\mathbf{c}_{k'} = \begin{cases} \mathbf{c}_1, & 0 \leq \eta \leq p(\mathbf{c}_1) \\ \vdots & \\ \mathbf{c}_k, & \sum_{i=1}^{k-1} p(\mathbf{c}_i) < \eta \leq \sum_{i=1}^{k} p(\mathbf{c}_i) \\ \vdots & \\ \mathbf{c}_K, & \sum_{i=1}^{K-1} p(\mathbf{c}_i) < \eta \leq 1 \end{cases}. \tag{8}$$

Note that performing K times of the above selection results K (not necessarily distinct) individuals.

D. CROSSOVER

After *selection*, pairs of the parent chromosomes $\mathbf{c}_i^{(\text{par})}$ and $\mathbf{c}_j^{(\text{par})}$, randomly recombine (*crossover*) with probability α, to generate two offspring chromosomes $\mathbf{c}_i^{(\text{off})}$ and $\mathbf{c}_j^{(\text{off})}$ as follows

$$\begin{cases} \mathbf{c}_i^{(\text{par})} = \left[[\mathbf{c}_i]_1, \cdots, [\mathbf{c}_i]_a, \cdots, [\mathbf{c}_i]_M\right]^T \\ \mathbf{c}_j^{(\text{par})} = \left[[\mathbf{c}_j]_1, \cdots, [\mathbf{c}_j]_a, \cdots, [\mathbf{c}_j]_M\right]^T \end{cases} \Downarrow \begin{cases} \mathbf{c}_i^{(\text{off})} = \left[[\mathbf{c}_i]_1, \cdots, [\mathbf{c}_j]_a, \cdots, [\mathbf{c}_j]_M\right]^T \\ \mathbf{c}_j^{(\text{off})} = \left[[\mathbf{c}_j]_1, \cdots, [\mathbf{c}_i]_a, \cdots, [\mathbf{c}_i]_M\right]^T \end{cases}, \tag{9}$$

where $a \in \{2, \ldots, M\}$ is randomly selected with equal probability, indicating the position of crossover in the chromosome.

E. MUTATION

After *crossover*, each of the K individuals randomly alternates a single bit with probability β as follows, which is known as *mutation*,

$$\mathbf{c}_i^{(\text{par})} = \left[[\mathbf{c}_i]_1, \cdots, [\mathbf{c}_i]_b, \cdots, [\mathbf{c}_i]_M\right]^T \Downarrow \mathbf{c}_i^{(\text{off})} = \left[[\mathbf{c}_i]_1, \cdots, [\mathbf{c}_i]'_b, \cdots, [\mathbf{c}_i]_M\right]^T, \tag{10}$$

where $[\mathbf{c}_i]'_b \neq [\mathbf{c}_i]_b$, and $b \in \{2, \ldots, M\}$ is randomly selected with equal probability, indicating the position of mutation in the chromosome.

F. SUMMARY

With the initial K individuals as the first generation, the genetic algorithm applies *selection*, *crossover*, and *mutation* iteratively, until some preset number of iterations I is achieved. The generated individuals in each iteration is known as a new *generation*. After the last generation of individuals are obtained, the individual with the greatest fitness is regarded as the optimized solution, i.e.,

$$\mathbf{c}_{opt} = \arg\max_{\mathbf{c}_k} \left\{f(\mathbf{c}_k)\right\}, \quad \text{for } k = 1, \ldots, K. \tag{11}$$

The steps of DOA classification with genetic algorithm is summarized in Table 1.

TABLE 1. Summary of DOA classification steps with genetic algorithm.

(S1)	Initialization	Randomly pick K columns from $\mathbf{C}_\ell$ in (4) as the first generation of individuals.
(S2)	Fitness evaluation	Evaluate the fitness of all individuals obtained in (S1) using equation (5).
(S3)	Selection	Perform K times of selection in (8), with the selection rates in (7).
(S4)	Crossover	For the neighboring individuals apply the crossover in (9), with the crossover rate α.
(S5)	Mutation	For each individual apply the mutation in (10), with the mutation rate β.
(S6)	Optimization	Iterate (S2) to (S6) for I times to obtain the last generation. Evaluate $\mathbf{c}_{opt}$ in (11).

IV. MULTIPLE SOURCES LOCALIZATION

With the initialization of $[\mathbf{c}]_1$, applying the algorithms in Sections III results only one group of classified directional rays steering to a single source of interest. To locate all L sources in the space, the aforementioned procedure should be carried out iteratively for L times.

For one specific $\mathbf{c}_{opt}$ obtained in (11), it corresponds to M directional rays $\left\{\mathbf{p}_m, \hat{\mathbf{u}}_{m,[\mathbf{c}_{opt}]_m}\right\}$, where $m = 1, \ldots, M$. The least square estimate of the corresponding source position can be obtained by [7], [9]

$$\hat{\mathbf{q}} = \left(M\mathbf{I} - \widehat{\mathbf{U}}\widehat{\mathbf{U}}^T\right)^{-1} \mathbf{A}\mathbf{w} \tag{12}$$

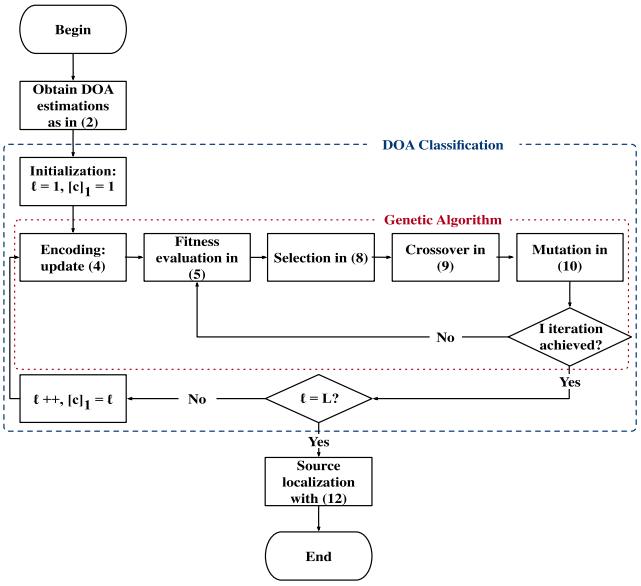

FIGURE 2. The flow chart of the proposed multiple source localization algorithm.

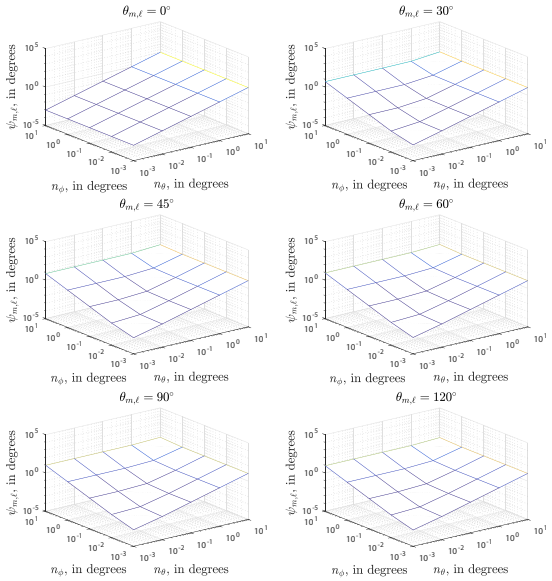

FIGURE 3. $\psi_{m,\ell}$ (as the vertical axis) against n_ϕ and n_θ (as the horizontal axes).

where $\mathbf{I}$ is the identity matrix with compatible size, $\widehat{\mathbf{U}} = \left[\widehat{\mathbf{u}}_{1,[\mathbf{c}_{opt}]_1}, \cdots, \widehat{\mathbf{u}}_{M,[\mathbf{c}_{opt}]_M}\right]$, $\mathbf{w} = [\underbrace{1, \cdots, 1}_{M}]^T$, and

$$\mathbf{A} = \left[\left(\mathbf{I} - \widehat{\mathbf{u}}_{1,[\mathbf{c}_{opt}]_1}\left(\widehat{\mathbf{u}}_{1,[\mathbf{c}_{opt}]_1}\right)^T\right)\mathbf{p}_1, \cdots, \left(\mathbf{I} - \widehat{\mathbf{u}}_{M,[\mathbf{c}_{opt}]_M}\left(\widehat{\mathbf{u}}_{M,[\mathbf{c}_{opt}]_M}\right)^T\right)\mathbf{p}_M\right].$$

V. OVERVIEW OF THE PROPOSED ALGORITHM

Concluding Sections III to IV, the proposed multiple sources localization algorithm is summarized in Figure 2.

VI. PERFORMANCE METRICS

A. ANGULAR ERROR

The direction vector $\mathbf{u}_{m,\ell}$ from the m-th sensor node to the ℓ-th source is modeled in equation (1), and its estimate is defined as $\hat{\mathbf{u}}_{m,\ell}$ in Section II. The angular error of $\mathbf{u}_{m,\ell}$ and $\hat{\mathbf{u}}_{m,\ell}$ can be thus defined by their in-between angle:

$$\begin{aligned}
\psi_{m,\ell} &\triangleq \arccos\left(\mathbf{u}_{m,\ell}^T\hat{\mathbf{u}}_{m,\ell}\right)\\
&= \arccos\Big(\sin\theta_{m,\ell}\cos\phi_{m,\ell}\sin\hat{\theta}_{m,\ell}\cos\hat{\phi}_{m,\ell}\\
&\quad + \sin\theta_{m,\ell}\sin\phi_{m,\ell}\sin\hat{\theta}_{m,\ell}\sin\hat{\phi}_{m,\ell}\\
&\quad + \cos\theta_{m,\ell}\cos\hat{\theta}_{m,\ell}\Big)\\
&= \arccos\Big[\sin\theta_{m,\ell}\sin\hat{\theta}_{m,\ell}\cos(\phi_{m,\ell} - \hat{\phi}_{m,\ell})\\
&\quad + \cos\theta_{m,\ell}\cos\hat{\theta}_{m,\ell}\Big]\\
&= \arccos\left[\cos(\theta_{m,\ell} - \hat{\theta}_{m,\ell})\cos^2\left(\frac{\phi_{m,\ell} - \hat{\phi}_{m,\ell}}{2}\right)\right.\\
&\quad \left. + \cos(\theta_{m,\ell} + \hat{\theta}_{m,\ell})\sin^2\left(\frac{\phi_{m,\ell} - \hat{\phi}_{m,\ell}}{2}\right)\right]\\
&= \arccos\left[\cos(n_\theta)\cos^2\left(\frac{n_\phi}{2}\right)\right.\\
&\quad \left. + \cos\left(2\theta_{m,\ell} + n_\theta\right)\sin^2\left(\frac{n_\phi}{2}\right)\right], \qquad (13)
\end{aligned}$$

where the fourth equality in (13) holds due to the trigonometric identities, n_θ and n_ϕ defined in equation (2). Apparently, the realization of $\psi_{m,\ell}$ depends on three degrees of freedom: $\theta_{m,\ell}$, the realization of n_ϕ, and the realization of n_θ. For specific $\theta_{m,\ell}$, Figure 3 plots $\psi_{m,\ell}$ in equation (13) against n_ϕ and n_θ. It is intuitive that $\psi_{m,\ell}$ increases as n_ϕ or n_θ increases.

Note that $\psi_{m,\ell}$ is random due to the random variables n_θ and n_ϕ. The statistics of $\psi_{m,\ell}$ can be hardly obtained in closed-form because of the complexity of equation (13). Alternatively, the average level of direction vectors' angular errors can be numerically assessed by the standard deviations of $\psi_{m,\ell}, \forall m, \forall \ell$

$$\overline{\sigma}_\psi \triangleq \frac{1}{ML}\sum_{m,\ell}\mathrm{Std}\left\{\psi_{m,\ell}\right\}. \qquad (14)$$

B. LOCALIZATION ERROR

For the ℓ-th source, define the absolute localization error as the Euclidean distance between the source's true location and its estimate, i.e., $\Delta_\ell = \|\hat{\mathbf{q}}_\ell - \mathbf{q}_\ell\|$. This absolute localization error may not be the best metric to assess the localization performance, because it depends on the distances from the sensors to the source, with even the same level of angular errors in (2).

To account for the spatial dimension that spanned by the ℓ-th source and all the M sensors, the average source-sensor

distance is defined as $\bar{d}_\ell \triangleq \frac{1}{M}\sum_{m=1}^{M}\|\mathbf{p}_m - \mathbf{q}_\ell\|$. The relative localization error is then suggested as $\delta_\ell \triangleq \Delta_\ell/\bar{d}_\ell$, for $\ell = 1, \cdots, L$. By considering all the L sources, the average relative localization error is proposed as

$$\bar{\delta} \triangleq \frac{1}{L}\sum_{\ell=1}^{L}\delta_\ell = \frac{1}{L}\sum_{\ell=1}^{L}\frac{\Delta_\ell}{\bar{d}_\ell} = \frac{1}{L}\sum_{\ell=1}^{L}\frac{\|\hat{\mathbf{q}}_\ell - \mathbf{q}_\ell\|}{\frac{1}{M}\sum_{m=1}^{M}\|\mathbf{p}_m - \mathbf{q}_\ell\|}. \quad (15)$$

Since the metric $\bar{\delta}$ is a random variable due to the random estimator $\hat{\mathbf{q}}_\ell$, N times independent Monte Carlo runs can be performed to evaluate the statistical average of $\bar{\delta}$.

VII. NUMERICAL RESULTS

A. PROPOSED ALGORITHM V.S. [36]

The proposed multiple sources localization method is based on the following essentials:

(i) the DOA classification with the genetic algorithm in Section III,
(ii) the close-form estimates of the multiple sources positions in Section IV.

To show the efficacy of multiple sources estimation, the proposed algorithm is compared with the localization strategy in [36], where the DOA classification in (i) is substituted by the *sequential-search* while (ii) remains unchanged.

Note that [36] searches for the global optimum of the DOA classification, while the proposed genetic algorithm guarantees only the suboptimal. Thus, in the noiseless case the proposed algorithm would not generally outperform [36] in terms of localization accuracy. In other word, [36] would readily serve as a benchmark for the proposed algorithm's accuracy.

In the simulations, $M = 6$ sensor nodes are deployed, with $L = 15$ sources distributed in the space. The spatial locations of the sensor nodes and the sources are summarized in Table 2. The proposed DOA classification with genetic algorithm has the parameters of $K = 300, \alpha = 0.7, \beta = 0.05$, $I = 120$, $w_1 = 0.8$, and $w_2 = 0.2$.

With the spatial positions of sensor nodes and sources presented in Table 2, the proposed algorithm is evaluated

TABLE 2. Spatial locations of the sensor nodes and the sources.

Sensor nodes					
$\mathbf{p}_1$	$\mathbf{p}_2$	$\mathbf{p}_3$	$\mathbf{p}_4$	$\mathbf{p}_5$	$\mathbf{p}_6$
$\begin{bmatrix}0.0\\4.5\\66.5\end{bmatrix}$	$\begin{bmatrix}62.3\\0.0\\42.9\end{bmatrix}$	$\begin{bmatrix}100.0\\74.5\\10.1\end{bmatrix}$	$\begin{bmatrix}32.2\\100.0\\70.4\end{bmatrix}$	$\begin{bmatrix}0.0\\16.6\\96.2\end{bmatrix}$	$\begin{bmatrix}62.7\\0.0\\5.2\end{bmatrix}$

Sources						
$\mathbf{q}_1$	$\mathbf{q}_2$	$\mathbf{q}_3$	$\mathbf{q}_4$	$\mathbf{q}_5$	$\mathbf{q}_6$	$\mathbf{q}_7$
$\begin{bmatrix}47.8\\54.5\\63.4\end{bmatrix}$	$\begin{bmatrix}36.2\\45.7\\59.8\end{bmatrix}$	$\begin{bmatrix}36.8\\40.2\\66.3\end{bmatrix}$	$\begin{bmatrix}43.3\\47.5\\60.1\end{bmatrix}$	$\begin{bmatrix}66.1\\36.7\\44.0\end{bmatrix}$	$\begin{bmatrix}47.7\\44.0\\25.9\end{bmatrix}$	$\begin{bmatrix}51.4\\39.3\\56.6\end{bmatrix}$

Sources							
$\mathbf{q}_8$	$\mathbf{q}_9$	$\mathbf{q}_{10}$	$\mathbf{q}_{11}$	$\mathbf{q}_{12}$	$\mathbf{q}_{13}$	$\mathbf{q}_{14}$	$\mathbf{q}_{15}$
$\begin{bmatrix}70.8\\43.1\\54.6\end{bmatrix}$	$\begin{bmatrix}60.4\\51.2\\36.0\end{bmatrix}$	$\begin{bmatrix}53.2\\73.8\\54.4\end{bmatrix}$	$\begin{bmatrix}42.0\\50.1\\39.8\end{bmatrix}$	$\begin{bmatrix}28.9\\60.7\\42.3\end{bmatrix}$	$\begin{bmatrix}37.6\\57.0\\32.7\end{bmatrix}$	$\begin{bmatrix}30.3\\46.1\\36.3\end{bmatrix}$	$\begin{bmatrix}54.0\\55.4\\42.1\end{bmatrix}$

TABLE 3. Localization statistics defined in Section VI-B, at $\bar{\sigma}_\psi \approx 0.4°$.

ℓ	1	2	3	4	5	6	7
Δ_ℓ	4.03	2.32	0.74	1.40	1.00	0.81	0.89
$\bar{d}_\ell$	67.56	64.46	64.37	64.94	65.24	66.55	63.55
$\delta_\ell = \frac{\Delta_\ell}{\bar{d}_\ell}$	5.96%	3.59%	1.15%	2.15%	1.53%	1.21%	1.40%

ℓ	8	9	10	11	12	13	14	15
Δ_ℓ	11.76	1.56	4.18	0.56	0.90	2.23	2.03	1.10
$\bar{d}_\ell$	68.62	67.41	73.81	65.46	69.79	69.03	66.23	67.23
$\delta_\ell = \frac{\Delta_\ell}{\bar{d}_\ell}$	17.14%	2.31%	5.66%	0.85%	1.28%	3.22%	3.06%	1.64%

at the average angular error of $\bar{\sigma}_\psi \approx 0.4°$. Δ_ℓ, $\bar{d}_\ell$, and δ_ℓ defined in Section VI-B for all 15 sources are calculated and summarized in Table 3. It can be seen that $\min\{\delta_\ell\} = 0.85\%$ and $\max\{\delta_\ell\} = 17.14\%$, which gives the average relative localization error of $\bar{\delta} = 3.48\%$.

The proposed multiple sources localization algorithm is compared with the *sequential-search* method in [36]. Figure 4a evaluates both algorithms' localization accuracy. The average relative localization error $\bar{\delta}$ against the standard deviation of angular error $\bar{\sigma}_\psi$ is shown with $N = 100$ Monte Carlo runs. It can be observed that the proposed algorithm results $\bar{\delta} \leq 5\%$ when $\bar{\sigma}_\psi \leq 0.5°$, which is only about 2 to 3 percentage points higher than the *sequential-search* method. As $\bar{\sigma}_\psi$ increases, $\bar{\delta}$ of both the proposed algorithm and the *sequential-search* method increases. And the performance gap between the two algorithms eventually decreases.

Figure 4b shows the average run time of the proposed algorithm and the *sequential-search* method in [36], where the simulations are conducted in a computer environment with Microsoft Windows 10.0.17134 operation system, Intel Core i7-8700 CPU @ 3.20GHz, and 24GB memory. It is shown that the run time of the proposed algorithm maintains a low level of around 6 seconds, which is only 22.2% of the *sequential-search* method's run time of roughly 27 seconds.

Figures 4a and 4b together indicate that the proposed algorithm greatly reduces 77.8% of the computation load by yielding no more than 3% of the localization accuracy.

B. FITNESS FUNCTION ON w_1 AND w_2

The fitness function (5) in Section III-B is designed as a weighted sum of Σ_1 and Σ_2. Note that Σ_1 assesses the closeness between a single directional ray $\{\mathbf{p}_1, \hat{\mathbf{u}}_{1,[\mathbf{c}]_1}\}$ and the rest $M-1$ directional rays $\{\mathbf{p}_m, \hat{\mathbf{u}}_{m,[\mathbf{c}]_m}\}$ where $m = 2, 3, \ldots, M$. On the other hand, Σ_2 assesses the closeness of the rest $M-1$ directional rays only. In this Section VII-B, numerical examples are shown to demonstrate the proposed algorithm's performance against different weighting strategy.

With the sources and sensor nodes described in Table 2, Figure 5a illustrates the localization performance of the proposed algorithm depending on various weighting strategies where the other algorithm parameters remain the same as in Figures 4a and 4b. As w_1 gets larger from $w_1 = 0.5$ to

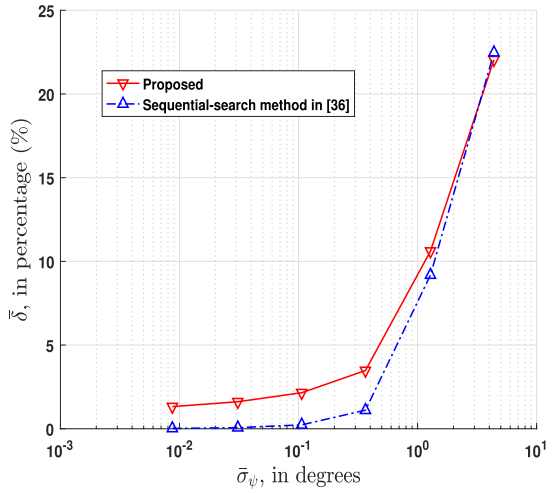

(a)

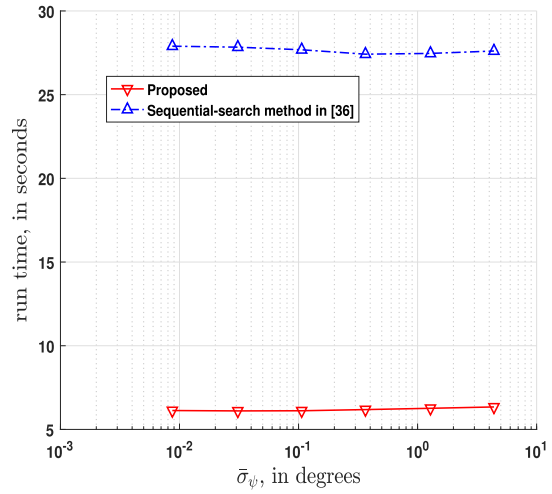

(b)

FIGURE 4. (4a) Estimation accuracy assessment in terms of $\bar{\delta}$, where $L = 15$, $M = 6$, $K = 300$, $\alpha = 0.7$, $\beta = 0.05$, $I = 120$, $w_1 = 0.8$, $w_2 = 0.2$, and $N = 100$. (4b) Computational complexity assessment in terms of algorithm time, where $L = 15$, $M = 6$, $K = 300$, $\alpha = 0.7$, $\beta = 0.05$, $I = 120$, $w_1 = 0.8$, $w_2 = 0.2$, and $N = 100$.

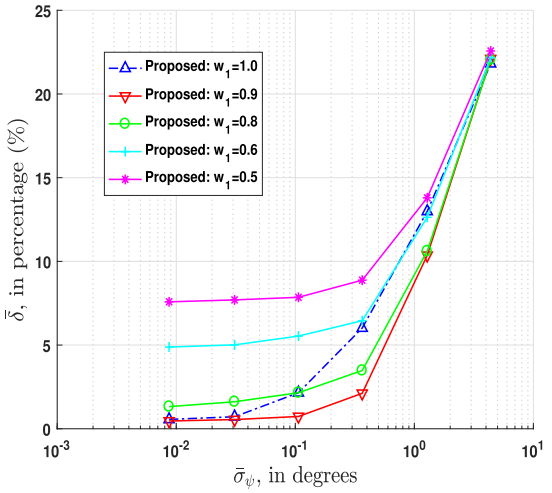

(a)

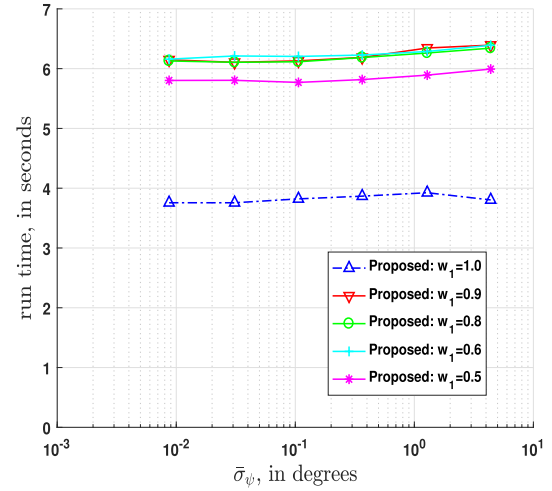

(b)

FIGURE 5. (5a) Estimation accuracy assessment in terms of $\bar{\delta}$, where $L = 15$, $M = 6$, $K = 300$, $\alpha = 0.7$, $\beta = 0.05$, $I = 120$, and $N = 100$. (5b) Computational complexity assessment in terms of algorithm time, where $L = 15$, $M = 6$, $K = 300$, $\alpha = 0.7$, $\beta = 0.05$, $I = 120$, and $N = 100$.

$w_1 = 0.9$, it can be observed that the localization accuracy improves as the overall level of $\bar{\delta}$ decreases. The improvement is especially significant when $\bar{\sigma}_\psi$ is relatively small (due to the weaker angular noise). This is intuitive, because the larger w_1 means Σ_1 is more dominant in (5), which helps to better classify the directional rays corresponding to the source concerned.

Comparing to the other values of w_1, the blue curve with $w_1 = 1$ shows a steeper increasing trend of $\bar{\delta}$ as $\bar{\sigma}_\psi$ increases. It implies that the localization accuracy with $w_1 = 1$ is more sensitive to the angular noise than the other weights. Note that the fitness function in (5) degenerates to $f(\mathbf{c}) = \Sigma_1^{-1}$ when $w_1 = 1$. The absence of Σ_2, which reflects the closeness of the rest of $M - 1$ directional rays, may cause the fitness being more vulnerable to the noise, thus less robustness of the algorithm.

Figure 5b compares the average run time of the proposed algorithm with different weighting strategy. From $w_1 = 0.5$ to $w_1 = 0.9$, the algorithm time does not vary much. On the other hand, the run time for $w_1 = 1$ is about 33% lower than the other weights. This is reasonable, because the computation of (5) for $w_1 = 1$ can be significantly reduced due to the absence of the double summation term Σ_2.

Figures 5a and 5b together indicate that, the weighting strategy with $w_1 = 0.9$ may be a good choice to offer robust and accurate localization estimates comparing to the other weights.

C. ALGORITHM PERFORMANCE AGAINST THE NUMBER OF SOURCES

Figures 6a and 6b compare the proposed algorithm with the *sequential-search* method in [36], against the number of

TABLE 4. Spatial locations of the sensor nodes and the sources.

Sensor nodes				
$\mathbf{p}_1$	$\mathbf{p}_2$	$\mathbf{p}_3$	$\mathbf{p}_4$	$\mathbf{p}_5$
$\begin{bmatrix}0.0\\4.5\\66.5\end{bmatrix}$	$\begin{bmatrix}62.3\\0.0\\42.9\end{bmatrix}$	$\begin{bmatrix}100.0\\74.5\\10.1\end{bmatrix}$	$\begin{bmatrix}32.2\\100.0\\70.4\end{bmatrix}$	$\begin{bmatrix}0.0\\16.6\\96.2\end{bmatrix}$

Sources						
$\mathbf{q}_1$	$\mathbf{q}_2$	$\mathbf{q}_3$	$\mathbf{q}_4$	$\mathbf{q}_5$	$\mathbf{q}_6$	$\mathbf{q}_7$
$\begin{bmatrix}47.8\\54.5\\63.4\end{bmatrix}$	$\begin{bmatrix}36.2\\45.7\\59.8\end{bmatrix}$	$\begin{bmatrix}36.8\\40.2\\66.3\end{bmatrix}$	$\begin{bmatrix}43.3\\47.5\\60.1\end{bmatrix}$	$\begin{bmatrix}66.1\\36.7\\44.0\end{bmatrix}$	$\begin{bmatrix}47.7\\44.0\\25.9\end{bmatrix}$	$\begin{bmatrix}51.4\\39.3\\56.6\end{bmatrix}$

Sources						
$\mathbf{q}_8$	$\mathbf{q}_9$	$\mathbf{q}_{10}$	$\mathbf{q}_{11}$	$\mathbf{q}_{12}$	$\mathbf{q}_{13}$	$\mathbf{q}_{14}$
$\begin{bmatrix}70.8\\43.1\\54.6\end{bmatrix}$	$\begin{bmatrix}60.4\\51.2\\36.0\end{bmatrix}$	$\begin{bmatrix}53.2\\73.8\\54.4\end{bmatrix}$	$\begin{bmatrix}42.0\\50.1\\39.8\end{bmatrix}$	$\begin{bmatrix}28.9\\60.7\\42.3\end{bmatrix}$	$\begin{bmatrix}37.6\\57.0\\32.7\end{bmatrix}$	$\begin{bmatrix}30.3\\46.1\\36.3\end{bmatrix}$

Sources						
$\mathbf{q}_{15}$	$\mathbf{q}_{16}$	$\mathbf{q}_{17}$	$\mathbf{q}_{18}$	$\mathbf{q}_{19}$	$\mathbf{q}_{20}$	$\mathbf{q}_{21}$
$\begin{bmatrix}54.0\\55.4\\42.1\end{bmatrix}$	$\begin{bmatrix}64.5\\49.7\\33.3\end{bmatrix}$	$\begin{bmatrix}37.9\\48.1\\69.9\end{bmatrix}$	$\begin{bmatrix}55.7\\40.5\\37.5\end{bmatrix}$	$\begin{bmatrix}42.6\\57.3\\58.5\end{bmatrix}$	$\begin{bmatrix}36.7\\49.5\\59.9\end{bmatrix}$	$\begin{bmatrix}42.1\\39.0\\32.4\end{bmatrix}$

Sources						
$\mathbf{q}_{22}$	$\mathbf{q}_{23}$	$\mathbf{q}_{24}$	$\mathbf{q}_{25}$	$\mathbf{q}_{26}$	$\mathbf{q}_{27}$	$\mathbf{q}_{28}$
$\begin{bmatrix}50.4\\72.1\\53.6\end{bmatrix}$	$\begin{bmatrix}71.2\\45.8\\59.6\end{bmatrix}$	$\begin{bmatrix}58.5\\43.9\\42.7\end{bmatrix}$	$\begin{bmatrix}38.1\\48.8\\56.8\end{bmatrix}$	$\begin{bmatrix}72.3\\39.7\\47.8\end{bmatrix}$	$\begin{bmatrix}72.9\\35.9\\59.3\end{bmatrix}$	$\begin{bmatrix}54.2\\34.5\\60.8\end{bmatrix}$

Sources				
$\mathbf{q}_{29}$	$\mathbf{q}_{30}$	$\mathbf{q}_{31}$	$\mathbf{q}_{32}$	$\mathbf{q}_{33}$
$\begin{bmatrix}40.9\\44.5\\63.2\end{bmatrix}$	$\begin{bmatrix}42.1\\49.7\\59.3\end{bmatrix}$	$\begin{bmatrix}62.4\\60.8\\47.0\end{bmatrix}$	$\begin{bmatrix}30.8\\48.5\\58.4\end{bmatrix}$	$\begin{bmatrix}67.1\\36.1\\46.8\end{bmatrix}$

TABLE 5. Spatial locations of the sensor nodes and the sources.

Sensor nodes						
$\mathbf{p}_1$	$\mathbf{p}_2$	$\mathbf{p}_3$	$\mathbf{p}_4$	$\mathbf{p}_5$	$\mathbf{p}_6$	$\mathbf{p}_7$
$\begin{bmatrix}0.0\\4.5\\66.5\end{bmatrix}$	$\begin{bmatrix}62.3\\0.0\\42.9\end{bmatrix}$	$\begin{bmatrix}100.0\\74.5\\10.1\end{bmatrix}$	$\begin{bmatrix}32.2\\100.0\\70.4\end{bmatrix}$	$\begin{bmatrix}0.0\\16.6\\96.2\end{bmatrix}$	$\begin{bmatrix}62.7\\0.0\\5.2\end{bmatrix}$	$\begin{bmatrix}100.0\\40.9\\61.3\end{bmatrix}$

Sensor nodes						
$\mathbf{p}_8$	$\mathbf{p}_9$	$\mathbf{p}_{10}$	$\mathbf{p}_{11}$	$\mathbf{p}_{12}$	$\mathbf{p}_{13}$	$\mathbf{p}_{14}$
$\begin{bmatrix}64.7\\100.0\\16.7\end{bmatrix}$	$\begin{bmatrix}0.0\\2.9\\9.6\end{bmatrix}$	$\begin{bmatrix}97.7\\0.0\\90.0\end{bmatrix}$	$\begin{bmatrix}100.0\\20.7\\17.7\end{bmatrix}$	$\begin{bmatrix}72.8\\100.0\\79.8\end{bmatrix}$	$\begin{bmatrix}0.0\\81.1\\87.5\end{bmatrix}$	$\begin{bmatrix}19.7\\0.0\\23.1\end{bmatrix}$

Sensor nodes						
$\mathbf{p}_{15}$	$\mathbf{p}_{16}$	$\mathbf{p}_{17}$	$\mathbf{p}_{18}$	$\mathbf{p}_{19}$	$\mathbf{p}_{20}$	$\mathbf{p}_{21}$
$\begin{bmatrix}100.0\\84.5\\25.3\end{bmatrix}$	$\begin{bmatrix}87.3\\100.0\\9.6\end{bmatrix}$	$\begin{bmatrix}0.0\\17.9\\67.0\end{bmatrix}$	$\begin{bmatrix}69.6\\0.0\\6.4\end{bmatrix}$	$\begin{bmatrix}100.0\\17.8\\19.0\end{bmatrix}$	$\begin{bmatrix}50.9\\100.0\\84.2\end{bmatrix}$	$\begin{bmatrix}0.0\\4.2\\8.8\end{bmatrix}$

Sensor nodes						
$\mathbf{p}_{22}$	$\mathbf{p}_{23}$	$\mathbf{p}_{24}$	$\mathbf{p}_{25}$	$\mathbf{p}_{26}$	$\mathbf{p}_{27}$	$\mathbf{p}_{28}$
$\begin{bmatrix}70.7\\0.0\\3.1\end{bmatrix}$	$\begin{bmatrix}100.0\\82.1\\56.8\end{bmatrix}$	$\begin{bmatrix}31.7\\100.0\\38.8\end{bmatrix}$	$\begin{bmatrix}0.0\\29.9\\27.2\end{bmatrix}$	$\begin{bmatrix}53.9\\0.0\\17.3\end{bmatrix}$	$\begin{bmatrix}100.0\\51.7\\34.4\end{bmatrix}$	$\begin{bmatrix}4.1\\100.0\\78.6\end{bmatrix}$

Sensor nodes						
$\mathbf{p}_{29}$	$\mathbf{p}_{30}$	$\mathbf{p}_{31}$	$\mathbf{p}_{32}$	$\mathbf{p}_{33}$	$\mathbf{p}_{34}$	$\mathbf{p}_{35}$
$\begin{bmatrix}0.0\\92.7\\46.5\end{bmatrix}$	$\begin{bmatrix}28.1\\0.0\\77.8\end{bmatrix}$	$\begin{bmatrix}100.0\\47.5\\73.9\end{bmatrix}$	$\begin{bmatrix}12.6\\100.0\\42.2\end{bmatrix}$	$\begin{bmatrix}0.0\\43.4\\63.8\end{bmatrix}$	$\begin{bmatrix}34.1\\0.0\\42.7\end{bmatrix}$	$\begin{bmatrix}100.0\\57.7\\97.3\end{bmatrix}$

Sensor nodes						
$\mathbf{p}_{36}$	$\mathbf{p}_{37}$	$\mathbf{p}_{38}$	$\mathbf{p}_{39}$	$\mathbf{p}_{40}$	$\mathbf{p}_{41}$	$\mathbf{p}_{42}$
$\begin{bmatrix}36.7\\100.0\\36.5\end{bmatrix}$	$\begin{bmatrix}0.0\\68.2\\12.1\end{bmatrix}$	$\begin{bmatrix}77.0\\0.0\\61.2\end{bmatrix}$	$\begin{bmatrix}100.0\\81.3\\92.8\end{bmatrix}$	$\begin{bmatrix}85.5\\100.0\\42.1\end{bmatrix}$	$\begin{bmatrix}0.0\\69.4\\74.9\end{bmatrix}$	$\begin{bmatrix}45.7\\0.0\\7.0\end{bmatrix}$

Sensor nodes							
$\mathbf{p}_{43}$	$\mathbf{p}_{44}$	$\mathbf{p}_{45}$	$\mathbf{p}_{46}$	$\mathbf{p}_{47}$	$\mathbf{p}_{48}$	$\mathbf{p}_{49}$	$\mathbf{p}_{50}$
$\begin{bmatrix}100.0\\29.3\\76.5\end{bmatrix}$	$\begin{bmatrix}56.3\\100.0\\50.4\end{bmatrix}$	$\begin{bmatrix}0.0\\29.5\\28.4\end{bmatrix}$	$\begin{bmatrix}15.8\\0.0\\89.6\end{bmatrix}$	$\begin{bmatrix}100.0\\39.8\\56.3\end{bmatrix}$	$\begin{bmatrix}69.6\\100.0\\36.3\end{bmatrix}$	$\begin{bmatrix}0.0\\45.7\\85.4\end{bmatrix}$	$\begin{bmatrix}92.8\\0.0\\9.0\end{bmatrix}$

Sources				
$\mathbf{q}_1$	$\mathbf{q}_2$	$\mathbf{q}_3$	$\mathbf{q}_4$	$\mathbf{q}_5$
$\begin{bmatrix}47.8\\54.5\\63.4\end{bmatrix}$	$\begin{bmatrix}36.2\\45.7\\59.8\end{bmatrix}$	$\begin{bmatrix}36.8\\40.2\\66.3\end{bmatrix}$	$\begin{bmatrix}43.3\\47.5\\60.1\end{bmatrix}$	$\begin{bmatrix}66.1\\36.7\\44.0\end{bmatrix}$

sources L increasing from 5 to 33. The sources are randomly distributed inside a sphere with radius of 25 meters centering at $[50, 50, 50]^T$. For $K = 50$, 100 and 200, $M = 5$ sensor nodes are used with the genetic algorithm parameters of $\alpha = 0.7$, $\beta = 0.05$, $I = 120$, $w_1 = 0.9$, and $w_2 = 0.1$. The spatial locations of the sources and the sensor nodes are shown in Table 4.

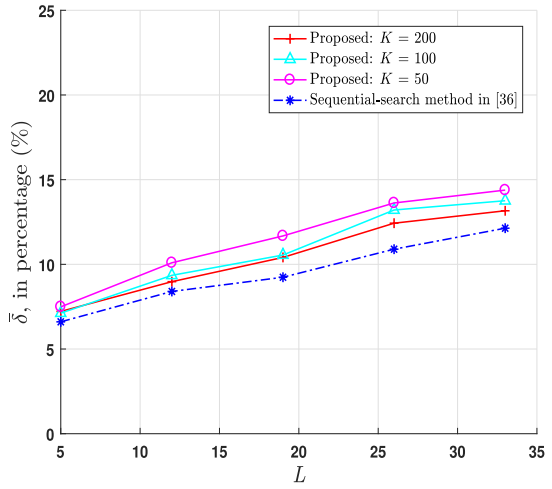

(a)

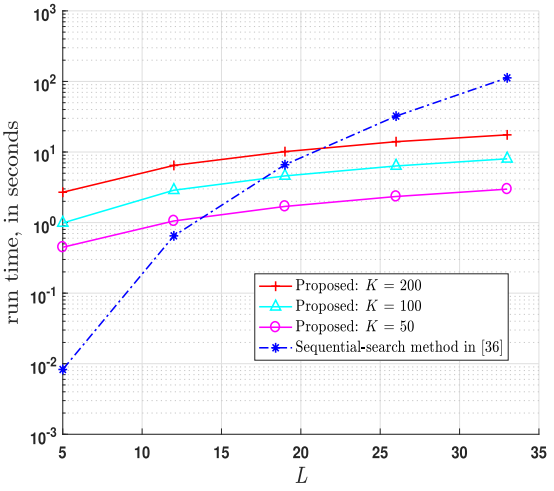

(b)

FIGURE 6. (6a) Estimation accuracy assessment in terms of $\bar{\delta}$, where $M = 5$, $\alpha = 0.7$, $\beta = 0.05$, $I = 120$, $w_1 = 0.9$, $w_2 = 0.1$ and $N = 100$. (6b) Computational complexity assessment in terms of algorithm time, where $M = 5$, $\alpha = 0.7$, $\beta = 0.05$, $I = 120$, $w_1 = 0.9$, $w_2 = 0.1$ and $N = 100$.

From Figure 6a, $\bar{\delta}$ of both methods increases as L increases, where the *sequential-search* method in [36] has the lowest overall level of $\bar{\delta}$. However, as K increases from 50 to 200, the proposed method eventually approaches [36]. The difference in $\bar{\delta}$ between the two methods can be within 2% for all L.

From Figure 6b, the run time of the proposed method increases as L increases, but much more slowly than that of [36]. When $L \geq 22$, the proposed method with $K = 50$, 100 and 200 significantly outperforms the *sequential-search* method in [36]. Moreover, as K increases from 50 to 200, the overall run time of the proposed method increases, which reflects the cost of having the better localization accuracy in Figure 6a.

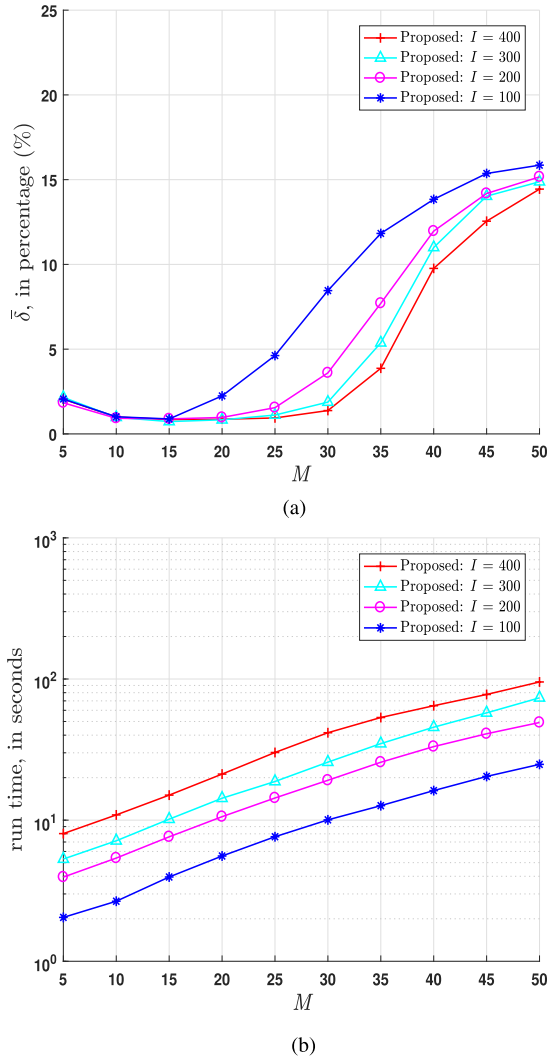

FIGURE 7. (7a) Estimation accuracy assessment in terms of $\bar{\delta}$, where $L = 5$, $\alpha = 0.7$, $\beta = 0.05$, $w_1 = 0.95$, $w_2 = 0.05$, $K = 200$ and $N = 100$. (7b) Computational complexity assessment in terms of algorithm time, where $L = 5$, $\alpha = 0.7$, $\beta = 0.05$, $w_1 = 0.95$, $w_2 = 0.05$, $K = 200$ and $N = 100$.

D. ALGORITHM PERFORMANCE AGAINST THE NUMBER OF SENSOR NODES

To assess proposed algorithm's performance against network scale, Figures 7a and 7b show the simulation results against increasing number of sensor nodes from 5 to 50, for $I = 100, 200, 300, 400$ iterations. In this scenario, $L = 5$ sources are to be located, where the proposed DOA classification have the genetic algorithm parameters of $\alpha = 0.7$, $\beta = 0.05$, $w_1 = 0.95$, $w_2 = 0.05$, and $K = 200$. The spatial locations of the sources and the sensor nodes are shown in Table 5.

From the simulation, the following insights can be drawn:

(i) From Figure 7a, $\bar{\delta}$ decreases and then increases as M increases from 5 to 50. It implies that increasing the number of sensor nodes may help, but not always, to locate the multiple sources more accurately to some extent. If M keeps increasing, $\bar{\delta}$ would eventually increases. This may be explained as follows. As M increases, the dimensions of *chromosome matrix* in equation (4) increases dramatically. The invariant setting of the genetic algorithm may eventually become ineffective to find the optimal solution. This phenomenon implies that it is not the best to deploy as many sensor nodes as possible.

(ii) For each curve in Figure 7a, a support range of M can be found where $\bar{\delta}$ does not dramatically vary, implying that the localization accuracy is relatively robust when the network scale increases. For $I = 100, 200, 300$ and 400, this range is roughly $M \in [5, 15]$, $M \in [5, 25]$, $M \in [5, 30]$, and $M \in [5, 30]$, respectively. This support range reflects the network size with which the algorithm is scalable.

(iii) Figure 7b shows that the run time monotonically increases as M increases. This is intuitive because the larger M means more summation terms to calculate the fitness function in (5) and (6).

(iv) In Figure 7a, the overall level of $\bar{\delta}$ decreases and the algorithm scalable range of M widens, as the number of iterations I increases. This is reasonable, because more iterations would increase the opportunity of the genetic algorithm to find the optimum solution. As a cost, more iterations results the heavier computation burden and longer algorithm run time, which is illustrated in Figure 7b.

VIII. CONCLUSION

With the direction-of-arrivals estimates obtained at each sensor node, proposed in this paper is a multiple sources localization method in the WSN. A DOA classification method is developed by using the genetic algorithm. The localization performance is compared with the conventional *sequential-search* method. Numerical results show that the proposed algorithm greatly reduces the computation load, by yielding little to the localization accuracy. The proposed algorithm has the advantages of the low computational load and inter-node communication burden, which could be especially suitable for the IoT applications with a large number of sources and/or sensor nodes.

REFERENCES

[1] J. H. Holland, *Adaption in Natural and Artificial Systems*. Cambridge, MA, USA: MIT Press, 1975.

[2] I. Ziskind and M. Wax, "Maximum likelihood localization of multiple sources by alternating projection," *IEEE Trans. Acoust., Speech Signal Process.*, vol. 36, no. 10, pp. 1553–1560, Oct. 1988.

[3] D. Whitley, "A genetic algorithm tutorial," *Statist. Comput.*, vol. 4, no. 2, pp. 65–85, Jun. 1994.

[4] B. Hofmann-Wellenhof, H. Lichtenegger, and J. Collins, *Global Positioning System: Theory and Practice*. Vienna, Austria: Springer-Verlag, 1997.

[5] K. I. Pedersen, P. E. Mogensen, and B. H. Fleury, "A stochastic model of the temporal and azimuthal dispersion seen at the base station in outdoor propagation environments," *IEEE Trans. Veh. Technol.*, vol. 49, no. 2, pp. 437–447, Mar. 2000.

[6] J. C. Chen, R. E. Hudson, and K. Yao, "Maximum-likelihood source localization and unknown sensor location estimation for wideband signals in the near-field," *IEEE Trans. Signal Process.*, vol. 50, no. 8, pp. 1843–1854, Aug. 2002.

[7] M. Hawkes and A. Nehorai, "Wideband source localization using a distributed acoustic vector-sensor array," *IEEE Trans. Signal Process.*, vol. 51, no. 6, pp. 1479–1491, Jun. 2003.
[8] X. Sheng and Y.-H. Hu, "Maximum likelihood multiple-source localization using acoustic energy measurements with wireless sensor networks," *IEEE Trans. Signal Process.*, vol. 53, no. 1, pp. 44–53, Jan. 2005.
[9] H. Liu and E. Milios, "Acoustic positioning using multiple microphone arrays," *Acoust. Soc. Amer.*, vol. 177, no. 5, pp. 2772–2782, Mar. 2005.
[10] X. Chen and U. Tureli, "Underwater source localization based on energy measurement with randomly distributed sensor array," *Proc. SPIE*, vol. 6562, May 2007, Art. no. 65620L.
[11] Q. Han, B. Hanna, and T. Ohira, "A compact espar antenna with planar parasitic elements on a dielectric cylinder," *IEICE Trans. Commun.*, vol. E88-B, no. 6, pp. 2284–2290, Jun. 2005.
[12] A. H. Sayed, A. Tarighat, and N. Khajehnouri, "Network-based wireless location: Challenges faced in developing techniques for accurate wireless location information," *IEEE Signal Process. Mag.*, vol. 22, no. 4, pp. 24–40, Jul. 2005.
[13] J. Lu, D. Ireland, and R. Schlub, "Dielectric embedded ESPAR (DE-ESPAR) antenna array for wireless communications," *IEEE Trans. Antennas Propag.*, vol. 53, no. 8, pp. 2437–2443, Aug. 2005.
[14] G. Mao, B. Fidan, and B. D. O. Anderson, "Wireless sensor network localization techniques," *Comput. Netw.*, vol. 51, no. 10, pp. 2529–2553, 2007.
[15] M. Li and Y. Lu, "Angle-of-arrival estimation for localization and communication in wireless networks," in *Proc. 16th Eur. Signal Process. Conf.*, Aug. 2008, pp. 1–5.
[16] M. Nilsson, "Localization using directional antennas and recursive estimation," in *Proc. 5th Workshop Positioning, Navigat. Commun.*, Mar. 2008, pp. 213–217.
[17] D. Ampeliotis and K. Berberidis, "Low complexity multiple acoustic source localization in sensor networks based on energy measurements," *Signal Process.*, vol. 90, no. 4, pp. 1300–1312, 2010.
[18] X. Shi and Y. Ma, "Weighted least square source localization theory in an underwater wireless sensor array network," in *Proc. 6th Int. Conf. Wireless Commun. Netw. Mobile Comput.*, Sep. 2010, pp. 1–4.
[19] W. Zhang, Q. Yin, and W. Wang, "Distributed angle estimation for wireless sensor network localization," in *Proc. IEEE Global Telecommun. Conf. (GLOBECOM)*, Miami, FL, USA, 2010, pp. 1–5. [Online]. Available: http://ieeexplore.ieee.org/stamp/stamp.jsp?tp=&arnumber=5683803&isnumber=5683069, doi: 10.1109/GLOCOM.2010.5683803.
[20] K. T. Wong, Y. I. Wu, and M. Abdulla, "Landmobile radiowave multipaths' DOA-distribution: Assessing geometric models by the open literature's empirical datasets," *IEEE Trans. Antennas Propag.*, vol. 58, no. 3, pp. 946–958, Mar. 2010.
[21] B. N. Hood and P. Barooah, "Estimating DoA from radio-frequency RSSI measurements using an actuated reflector," *IEEE Sensors J.*, vol. 11, no. 2, pp. 413–417, Feb. 2011.
[22] L. Lu, H.-C. Wu, K. Yan, and S. S. Iyengar, "Robust expectation-maximization algorithm for multiple wideband acoustic source localization in the presence of nonuniform noise variances," *IEEE Sensors J.*, vol. 11, no. 3, pp. 536–544, Mar. 2011.
[23] W. Meng, W. Xiao, and L. Xie, "An efficient EM algorithm for energy-based multisource localization in wireless sensor networks," *IEEE Trans. Instrum. Meas.*, vol. 60, no. 3, pp. 1017–1027, Mar. 2011.
[24] J. Wendeberg, T. Janson, and C. Schindelhauer, "Self-localization based on ambient signals," *Theor. Comput. Sci.*, vol. 453, pp. 98–109, Sep. 2012.
[25] Y. Zhang, S. Liu, and Z. Jia, "Localization using joint distance and angle information for 3D wireless sensor networks," *IEEE Commun. Lett.*, vol. 16, no. 6, pp. 809–811, Jun. 2012.
[26] S. Astapov, J.-S. Preden, and J. Berdnikova, "Simplified acoustic localization by linear arrays for wireless sensor networks," in *Proc. Int. Conf. Digit. Signal Process.*, Jul. 2013, pp. 1–6.
[27] W. Zhang, Q. Yin, H. Chen, F. Gao, and N. Ansari, "Distributed angle estimation for localization in wireless sensor networks," *IEEE Trans. Wireless Commun.*, vol. 12, no. 2, pp. 527–537, Feb. 2013.
[28] S. Astapov, J. Berdnikova, and J.-S. Preden, "A method of initial search region reduction for acoustic localization in distributed systems," in *Proc. 20th Int. Conf. Mixed Design Integr. Circuits Syst.*, Jun. 2013, pp. 451–456.
[29] L. Cheng, Y. Wang, C. Wu, H. Wu, and Y. Zhang, "Signal processing for a positioning system with binary sensory outputs," *Sens. Actuator A, Phys.*, vol. 201, pp. 86–92, Oct. 2013.
[30] H. Jamali-Rad and G. Leus, "Sparsity-aware multi-source TDOA localization," *IEEE Trans. Signal Process.*, vol. 61, no. 19, pp. 4874–4887, Oct. 2013.
[31] Y. I. Wu, H. Wang, and X. Zheng, "WSN localization using RSS in three-dimensional space—A geometric method with closed-form solution," *IEEE Sensors J.*, vol. 16, no. 11, pp. 4397–4404, Jun. 2016.
[32] T. J. S. Chowdhury, C. Elkin, V. Devabhaktuni, and D. B. Rawat, "Advances on localization techniques for wireless sensor networks: A survey," *Comput. Netw.*, vol. 110, pp. 284–305, Dec. 2016.
[33] S. Tomic, M. Beko, R. Dinis, and P. Montezuma, "Distributed algorithm for target localization in wireless sensor networks using RSS and AoA measurements," *Pervasive Mobile Comput.*, vol. 37, pp. 63–77, Jun. 2017.
[34] X. Wu and Z. Gu, "A joint time synchronization and localization method without known clock parameters," *Pervasive Mobile Comput.*, vol. 37, pp. 154–170, Jun. 2017.
[35] T.-N. Zhang, X.-P. Mao, Y.-M. Shi, and G.-J. Jiang, "An analytical subspace-based robust sparse Bayesian inference estimator for off-grid TDOA localization," *Digit. Signal Process.*, vol. 69, pp. 174–184, Oct. 2017.
[36] Y. I. Wu, "Multiple sources localization with WSN, eliminating the direction-of-arrival ambiguity symmetric with respect to the planar array," *IEEE Access*, vol. 6, pp. 46290–46296, Aug. 2018.

YUAN ZHANG received the B.Eng. degree in software engineering from Sichuan University, Chengdu, Sichuan, China, in 2018, where she is currently pursuing the M.Eng. degree in computer science.

YUE IVAN WU (S'08–M'10–SM'18) received the B.Eng. degree in communication engineering and the M.Eng. degree in communication and information system from the University of Electronic Science and Technology of China, Chengdu, Sichuan, China, in 2004 and 2007, respectively, and the Ph.D. degree in electronic and information engineering from the Hong Kong Polytechnic University, in 2018.

He was a Postdoctoral Fellow or a Research Fellow from the Hong Kong Polytechnic University, in 2011 and from 2015 to 2016. He was a Lecturer with the University of Electronic Science and Technology of China, from May 2010 to June 2013. He joined VALENS at Nanyang Technological University, Singapore, as a Research Fellow, in June 2011, and then the University of Florida, Gainesville, Florida, USA, as a Postdoctoral Associate, in July 2012. Since July 2013, he has been an Associate Professor with the College of Computer Science, Sichuan University, Chengdu. He is currently the Project Director with the Department of Information Science, National Natural Science Foundation of China (NSFC). His research interests include space-time signal processing, wireless sensor networks, and wireless channel modeling. Dr. Wu is on the editorial boards of the *IET Signal Processing*, IEEE Access, and the *Telecommunication Systems*.